Behind the Scenes on the Search for Neutrinoless Double-Beta Decay

Hava Schwartz[1]

***Abstract*— This paper aims to display a small fraction of the work done behind the scenes to contribute to a large-scale collaboration experiment. More specifically, it will display the learnings of a summer REU student at the University of Washington, working under Jason Detwiler with the Majorana Project, and how such work exemplifies the painstaking detail-oriented investigations that are required by such large-scale, sensitive experiments.**

I. INTRODUCTION

A. Motivations of the Majorana Collaboration

A difficult endeavor with grand implications, the Majorana Project is an experiment to search for neutrinoless double-beta decay of Germanium-76.[1] Recently discovered to possess mass, neutrinos are neutral fermions and are only known to participate in weak interactions, with three flavors: the electron neutrino, muon neutrino, and tau neutrino. In $\beta-$ decay, a nucleus transitions from a Z to a Z+2 state, releasing an electron and a right-handed electron antineutrino in the process. The measurement of neutrinoless double-beta decay would imply that the two electron antineutrinos annihilate one another before exiting the nucleus, confirming the neutrino to be a Majorana particle - a fermion that is its own antiparticle. In addition to determining the absolute scale of the neutrino mass, the Majorana experiment and other efforts of its ilk could make strides in the understanding of beyond standard model physics.

B. Importance of Background Noise Reduction

Though the objectives of the search are well-defined, the difficulty of the exploit can be equated to that of finding a needle in a hay stack, or rather observing a molehill on top of a mountain. There are many radiations that span over our region of interest, and identifying and eliminating these red herrings along with improving energy resolution of the detectors will improve the efficiency - the ratio of detected events to actual events - of the experiment significantly, until the detection of the rare ($0\nu\beta\beta$) event is possible. To understand this further, work was done with surface-level background γ radiation spectra to identify all major count peaks, and then to observe the effectiveness of lead shielding in the reduction of such backgrounds. Information from this analysis could be used to extract more details from previous data sets that were collected before clean, purified hardware was installed to the demonstrator, reducing commonly-found nuclear decays.

*This work was supported by the NSF University of Washington REU Program.

[1]Hava Schwartz is an Undergraduate in Physics at Stanford University

In addition to data analysis and processing, steps can be taken in the hardware setup to reduce background noise pollution. An example of this, work was done to design and create a mass-scale that would dampen vibrations in efforts to improve the isolation of a prototype detector from ground vibrations, such as those caused by foot traffic nearby. The prototype has previously rested on a commercial scale in order for the user to identify the volume of liquid nitrogen left in the apparatus, but with the addition of a new α detector to the setup, it will be even more top-heavy, magnifying this background.

II. CONTRIBUTIONS AND EXAMPLES OF DETAIL-ORIENTED INVESTIGATIONS IN BACKGROUND REDUCTION

As technology advances, experimental observations of physical phenomena require such precision that eliminating background and confounding data has become an almost impossible task. In result, in every detail of an experimental procedure, steps must be taken to investigate ways in which the sensitivity of the data collection could be improved. For large-scale experimental collaborations, such as MAJORANA, such detail-oriented steps are taken even far before and far after the time of data collection. Following are two examples of this.

A. Background Spectrum Analysis

Exemplifying the work that can be done long after the time of data collection, smaller scale data collections can be done to find patterns and quantify effects at a smaller cost than full runs. Here, we have utilized an old detector to measure surface-level γ radiation count energy spectra, with the hopes of using this information to quantify the effects of shielding as well as to identify and eliminate sources of background in data sets taken by Majorana Demonstrator before radiation-decontaminated hardware could be installed.

1) Detector and Shielding: Located at the Center for Experimental Nuclear Physics and Astronomy (CENPA) on the campus of University of Washington, C1 is a Reverse Electrode coaxial Germanium (REGe) detector. The measured γ radiation results from $\beta-$ decays, and is constantly occurring amongst the plethora of radioactive isotopes existing in the materials around us. Most prevalently, the decay chains of ^{232}Th, ^{238}U, and ^{40}K, account for a majority of the largest energy peaks in the spectrum. These isotopes were here at the time of the formation of the Earth, expected to have come from high-energy supernovae that created the cosmic dust from which our solar system emerged. Though radioactive, the mentioned isotopes possess half-lives that are on the

order of magnitude of the age of the planet, so they are still abundant today.

When gamma radiation enters C1, atoms of the Germanium detector are ionized by the incident radiation as well as radiation resulting from further Compton scattering. A bias voltage then separates the electron-hole pairs, pushing the electrons toward the p-contact at the outside of the cylindrical conductor, and the holes toward the n-contact, at the center of the semiconductor. This flow of charge, otherwise known as current, is then measured and amplified by a digitizer card. The height of this pulse is related to the energy of the ionizing radiation, so, by calibrating the device, the energy of the incident γ can be quantified.

The goal of shielding the detector is to prevent incident radiation from entering. To this end, lead bricks were added around the detector in layers, and new spectra were measured after the addition of each layer. An initial layer was placed on the ground beneath the apparatus, then a second and third layer act as walls covering the sides, and a fourth layer sits above as a roof on the detector.

2) Procedure and Data: The road to attaining useful information from surface-level γ radiation spectra observed by C1 began with identifying the origin of the radiation with energy corresponding to each of the discrete peaks. Trends in the data show noticeable "shoulders" to the left of the largest peaks, in which the base - from which the peaks stand out - is shifted due to the spread in energies of the Compton-scattered photons. The measured spectrum is first calibrated using the two largest peaks which are known to be at 1460keV from the decay of ^{40}K, and at 2614.5keV from the decay of ^{208}Tl which is on the decay chain of ^{232}Th.

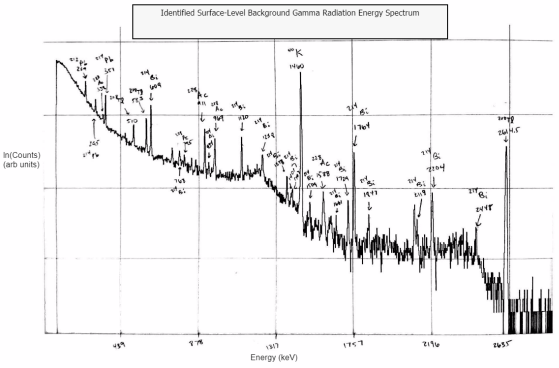

Fig. 1. Unshielded Surface-Level γ-Radiation Spectrum: Note the logarithmic scaling of the counts.

Following calibration, each step of the decay chains of ^{232}Th, ^{238}U, and ^{40}K is combed through meticulously, matching the most abundant γ emission energies with the peaks found in the spectrum. This process is repeated to ensure consistency. One such analyzed plot is shown in figure 1, in which major peaks are labeled with their energies and with the isotope from which that γ emission most likely came. The relative magnitudes of identified incident radiation peaks can be used to further filter out background from noisy data sets collected by the Majorana Demonstrator before purified, ultra-clean hardware was installed in the apparatus.

After the identification of the major radiation count peaks, the question arises: how effective is passive shielding at eliminating background γ radiation? By placing passive shielding, in the form of lead bricks, around the apparatus, we are able to identify characteristics of the shielding process that could help with the further filtering of data sets.

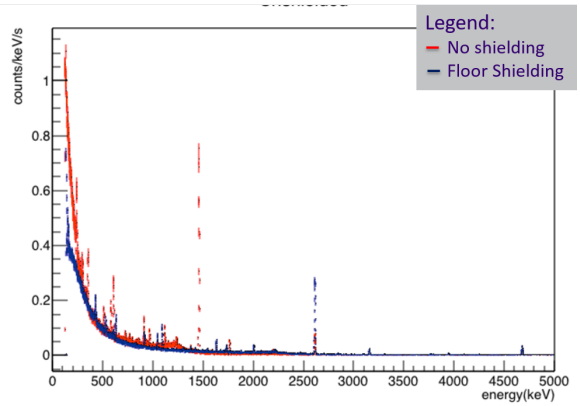

Fig. 2. Overlaid Comparison of γ-Radiation Spectra with No Shielding and with Floor Shielding Only[2]: Note the linear scaling of the counts.

[2]

Taking spectral data after the placement of each layer allows us to investigate the fraction of incident radiation blocked at each step. Figure 2 shows a comparison between a spectrum taken with no shielding and one with only floor shielding. Notice the generic reduction in amplitude of counts per unit time period across the domain, as to be expected. More interestingly, we notice that some peaks, many of which belong to the ^{40}K decay chain, disappear nearly completely with just floor shielding. This may suggest that the source of those peaks is primarily in the earth below the detector, and not as prevalent in the surrounding walls and other materials. However, it would be tough to make such conclusions with only this volume of data.

Furthering the shielding of the detector, we see the amplitude of radiation counts over a unit time period continue to diminish. Figure 3 illustrates this comparison. We see a comparable reduction due to the floor shielding, 2 layers of shielding, and 3 layers of shielding, with the frequency of incident radiation events reduced to almost half. The 4th layer encloses the detector, and reduces said frequency even further to just a small fraction of the unshielded equivalent. However, passive lead shielding, even when completely enclosing the detector, is not enough to reduce background radiation to 0, demonstrating why it is so important to consider background reduction in every detail of the experimental design.

[2]Graphs by Zachary Wuthrich, Undergraduate at University of Washington

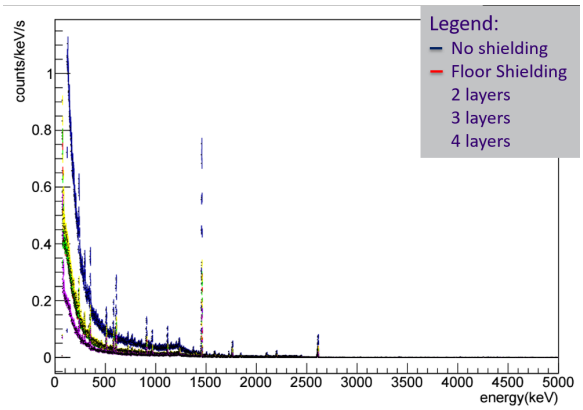

Fig. 3. Overlaid Comparison of γ-Radiation Spectra with Variable Shielding[2]: Note the linear scaling of the counts.

B. Vibration Resistance Mass Scale

As previously mentioned, efforts to mechanically eliminate background noise in hardware can be just as important as analytic and electronic reductions. Exemplifying this, an unexpected magnitude of mechanical vibrations were affecting the readouts of a prototype detector, in use for scale testing of future Majorana Project initiatives. It was determined that the mass scale, on which the detector apparatus sits, contributed largely to this noise. With plans to attach an α radiation detector to the top of the apparatus, further increasing the top-heaviness of the setup, the need to address this issue became more prevalent than ever. To this end, the effort was made to redesign a mass scale that would be vibration resistant and could replace the current tool.

1) Design Considerations: In alignment with form meeting function, the first step in the design process is an analysis of the goals of the exploit. The scale will serve to measure the weight of the apparatus, so as to alert the user of the volume of liquid nitrogen remaining in the chamber. For this purpose, the scale will need to operate in a range of roughly 70kg to 120kg. While the consistency of device measurement will be important, the precision and accuracy of the scale do not hold huge value, as the relevant information simmers down to whether the apparatus is full or empty of liquid nitrogen. As a result, our calculations do not need to be particularly precise, and fabrication will be much more practical.

[3]

In order to limit oscillatory motion of the scale, it will be important for it to be as solid as possible. For the measurement of the weight, force-sensitive resistors (FSR) will respond to changes in pressure from the weight atop by changing resistivity. With increased force, the material demonstrates a significant decrease in resistivity, ranging in resistance from many MOhms to less than an Ohm. Figure 4(a) shows the model used, which has a square force-sensing area measuring 38mm on each side. With the assistance of a simple voltmeter, the weight can be extrapolated. As depicted in Figure 4(b) and 4(c), four of these resistors will

[3]Interlink Electronics

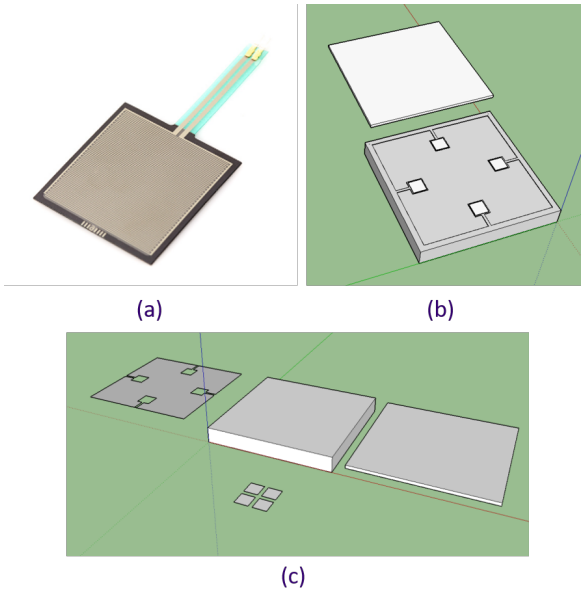

Fig. 4. (a) FSR 406[3]; (b) Design of mass scale with layers stacked; (b) A deconstructed view of each component of mass scale design.

sit between two aluminum plates, distributing the pressure among them equally. In order to put the weight range of needed purpose into the appropriate range of the force pads, it will be necessary for the weight to be spread across a larger area than just the FSR contact pads. Thus, a thin layer of rubber will surround the pads and fill in the rest of the space between the aluminum plates. In order for the pressure on the pads to be in their optimum working range, it was calculated that a surface area of about 1000cm^2 was necessary according to the operating specifications disclosed by the manufacturers of the FSR 406, Interlink Electronics. Nonetheless, due to differences in operating parameters of the force-sensitive resistors and imperfections in design fabrication, the dimensions for the final prototype were chosen to be 40cm on each side, giving a larger surface area. Lastly, it was found that the pressure pads possess a hard ”lip” that lines the perimeter, making it impossible for a flat object to compress the sensitive area of the pad. To combat this, thin incompressible squares will sit atop the force-sensing material, to allow contact with the aluminum plates. The four resistors will be connected in series, such that a single resistance measurement can be taken.

2) Prototypes and Adaptations: With the necessary design considerations taken into account, the prototype phase is also a phase in which hardware can be redesigned. Prototypes 1 and 2 are scale models, in which only one pressure pad was placed for testing. Figure 5 shows the results of these measurements.

Generation 1 was a square model, measuring 15cm on each side, intended to simulate the equivalent pressure of the 30cm original design for a single pressure pad. Looking at its performance in Figure 5, we are unable to recognize a significant trend in resistance with the addition of test weights. The spread in repeated measurements was too close to the change

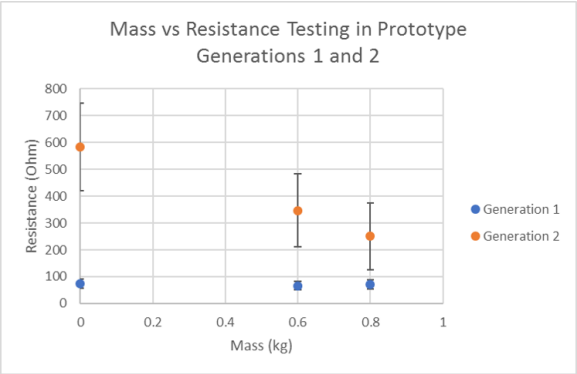

Fig. 5. Resistance Output vs. Mass Placed on Top of Scale for Reduced Size Prototypes 1 and 2

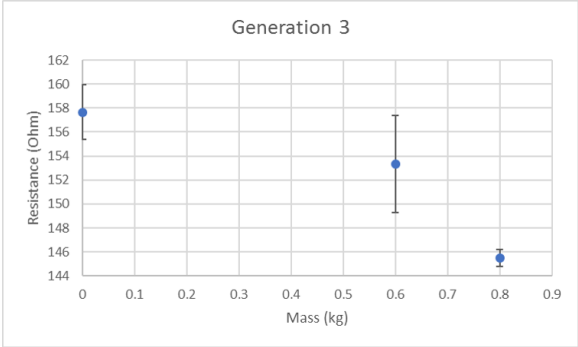

Fig. 6. Average Resistance Output per FSR vs. Mass Placed on Top of Scale for Full-Scale Prototype 3

in resistance due to mass differences. Additionally, while the magnitude of the resistance is not particularly relevant as the device can be calibrated to any resistance range, the test weights are much lighter than the weights that the sale would have to measure, so it is concerning the resistance measurements of Generation 1 are so low, less than 100 Ohms. When larger weight is placed on this device, it will lose too much sensitivity, as the resistance becomes too low to measure significant change. It was previously calculated that the surface area of the scale had to be around 1000 cm^2; however, due to differences in operating sensitivity ranges of the force-sensitive resistors and to imperfections in manufacturing and fabrication that lessen the surface area contact between the two plates, further prototypes utilize a larger working surface area.

Incorporating knowledge gained from the first prototype, Generation 2 was another scaled model measuring 20cm on each side, to fit a single force-sensitive resistor. Evident from the adjusted resistance outputs of Generation 2 in Figure 5, the added surface area shifted the device's sensitivity into working range. Nonetheless, repeated measurements show wild deviations in resistance output for the same mass, which would make consistency of the device minimal. Qualitative observations of these deviations showed a large correlation in placement position of the test masses on the top plate of the prototype. It is believed that this was caused by the roughness and unevenness of the surfaces of the metal plates, such that the pressure cannot spread evenly. A milling process to smooth the metal plates was therefore incorporated for future prototypes.

The third and final prototype as well as the first full-scale model, Generation 3 measures 40 cm on each side, fitting all four force-sensitive resistors, connected in series. The inner surfaces of the two metal plates have been milled for evenness, and the bottom plate will sit on vibration isolating pads, to maximize vibration dampening further, though no official studies on the effectiveness of the scale at dampening mechanical vibrations in comparison to the previous mass scale in use for the detector. Figure 6 displays the results of the placement of test masses repeatedly on the top plate of the device. Note that the shown outputs are averaged between the four sensors and not the combined total. The outputs show improved consistency with repeated measurements due to the milled surface, and the extended suraface area for force dispersion push the sensitivity of the sensors into our working range. Qualitatively, there was a "wobble" between the two plates, causing more pressure to be placed on one side and less on the opposite. It is believed that this defect could be improved with the addition of the compressible rubber padding between the plates.

In order to convert the Generation 3 prototype into a workable mass scale, further measurements must be taken to create calibration standards. Additionally, observations should be made of the effectiveness of the design at vibration dampening, once the isolation pads are installed to the bottom plate. Vibrations that are not dampened have been shown in the past to interrupt the baseline of the detector, essentially rendering any data collected during the time frame of those vibrations useless. For reasons such as this, it is evident that continuously redesigning and reworking even the simplest of mechanical components in a setup is integral to a maximally efficient experiment.

III. SUMMARY

Two concrete examples of the iterative, investigative process necessary to eliminate background noise in even the finest minutia of large-scale sensitive experimentation have been shown in this paper. Steps such as these are mandated at every stage of projects like Majorana.

ACKNOWLEDGMENT

Extreme gratitude to Jason Detwiler, Julieta Gruszko, Nick Ruof, Sebastian Alvis, Ian Guinn, Micah Buuck, Walter Pettus, and Zachary Wutherich at CENPA, for all of their guidance and tutelage. Thank you to Gray Rybka, Subhadeep Gupta, Cheryl McDaniel, Linda Vilett, and the NSF. Special thanks to Ron Musgrave for his never-ending patience. Lastly, a warm appreciation to my fellow University of Washington REU cohort for the pleasure of learning beside you.

REFERENCES

[1] Interlink Electronics. "FSR 400 Series Data Sheet." http://www.interlinkelectronics.com/datasheets/Datasheet_FSR.pdf.

[2] Knoll, Glenn. *Radiation detection and measurement.* New York: Wiley, 2000.
[3] ”MAJORANA.” The MAJORANA Neutrinoless Double-beta Decay Experiment — MAJORANA. https://www.npl.washington.edu/majorana/majorana-experiment.
[4] ”Uranium and Thorium decay chains.” http://hepwww.rl.ac.uk/ukdmc/radioactivity/uth_chains.html.